

Asymptotic Opening Angles for Colliding-Wind Bow Shocks: the Characteristic-Angle Approximation

Kenneth G. Gayley

University of Iowa, 203 Van Allen Hall, Iowa City, IA, 52245

ABSTRACT

By considering the advection and interaction of the vector momentum flux in highly supersonic spherically diverging winds, we derive a simple analytic description of the asymptotic opening angle of a wind-collision shock cone, in the approximation that the shocked gas is contained in a cone streaming out along a single characteristic opening angle. Both highly radiative and highly adiabatic limits are treated, and their comparison is the novel result. Analytic closed-form expressions are obtained for the inferred wind momentum ratios as a function of the observed shock opening angle, allowing the conspicuous shape of the asymptotic bow shock to be used as a preliminary constraint on more detailed modeling of the colliding winds. In the process, we explore from a general perspective the limitations in applying to the *global* shock geometry the so-called Dyson approximation, which asserts a local balance in the perpendicular ram pressure across the shock.

1. Introduction

Wind collisions in close binary systems provide a key laboratory for studying astrophysical shocks, including X-ray generation, particle acceleration, and dust creation. They also provide a unique opportunity to study the attributes of those winds via their hydrodynamical interaction, and it is this latter advantage that we explore here. Simulations (e.g., Girard & Willson 1987; Shore & Brown 1988; Eichler & Usov 2003) and observations (e.g., Hill, Moffat, & St-Louis 2002; Rauw et al. 2005; Ignace, Bessey, & Price 2009) both indicate that the interaction region forms a large-scale shock cone whose opening angle is diagnostically significant for the parameters of the wind interaction. Spectral diagnostics in emission or absorption (Luhrs 1997; St-Louis, Willis, & Stevens 1993; St-Louis et al. 2005), and the conspicuous formation of dusty “pinwheels” (Tuthill et al. 2008), make it feasible to use the shock opening angle as a constraint on the wind interaction.

The primary attribute of the winds that control this diagnostic is evidently their momentum-flux ratio, subject to the relative efficiency of radiative and adiabatic cooling. We certainly expect that the shock cone is narrower the greater the contrast between weak-wind and strong-wind momentum flux, and short radiative cooling times should also narrow the cone by minimizing the explosiveness of the interaction. Thus, a simple unified description of how these factors are

manifested in the asymptotic bow-shock angle is a particularly straightforward way to extract diagnostic information about these wind attributes.

Although sophisticated modeling, both numerical (Girard & Willson 1987; Shore & Brown 1988; Comeron & Kaper 1998) and analytical (Wilkin 1996; Canto, Raga, & Wilkin 1996; Pilyugin & Usov 2007), has been carried out in both radiative and adiabatic colliding-wind scenarios, no generalized treatment exists that can extend simple analytic results for the asymptotic opening angle to both the highly radiative and highly adiabatic limits. Certainly, fully detailed results are needed to determine X-ray flux diagnostics and the complete shock structure, but if we restrict attention to the asymptotic opening angle, a conspicuously observable diagnostic, then these various types of models may be analyzed in a simple way that underscores key physical differences in these limits. This is particularly convenient at early stages of analyzing a particular colliding-wind system, when it may not yet be clear which regime to expect.

When radiative cooling is so efficient that gas pressure never plays an important role in the global shock dynamics, one expects the “thin-shock approximation” (Girard & Willson 1987) to provide an adequate treatment, and in that case fully analytic results for the asymptotic opening angle were developed elegantly by Canto, Raga, & Wilkin (1996; hereafter CRW). However, this work has not yet been generalized to the opposite limit of slow cooling, and making that extension for either mixed or unmixed winds is the purpose of this paper. Neither approximation is without difficulties, as radiating shocks are subject to instabilities (Stevens, Blondin, & Pollack 1992) and adiabatically shocked gas streams will not remain confined to a thin layer owing to explosive expansion (Pittard 2007), but nevertheless the analytic results give a point of reference that informs more detailed and physically realistic simulations. Having access to simple closed-form results in both limits makes each more useful, by virtue of the implied contrasts between them.

1.1. The standard approach to the steady thin-shock geometry

When numerical results, rather than analytic forms, for the shape of a thin and steady shock are desired, the standard approach for determining the shock opening angle involves a detailed integration of the shock conditions all along its surface, starting from the stagnation point along the symmetry axis (when coriolis effects are neglected). The physical requirement for such an integration is that the shock cone has a “memory” of the history of the gas that it is carrying, encoded in the form of the mass, energy, and momentum fluxes along the shock cone, and the point where any windstream from one of the stars meets the working surface of the shock cone depends on that complete history— it is not a local attribute of that windstream. However, a simplification can be applied if it is only the *asymptotic* opening angle that is desired, not the detailed structure. Then the result should be expressible in a global form, breaking from the standard locally integrated numerical approach, and allowing the problem to be solved in a single step.

In other words, the opening angle should be solvable by applying purely global constraints,

but so far that has only been possible for highly radiative thin shocks, as assumed in CRW. We suggest that a systematic, if idealized, approximation that allows for such global constraints follows from a simple extension of the thin-shock approximation to include adiabatic cooling, but which conserves different wind properties consistent with the presence of explosive gas pressure and the absence of significant radiative cooling. Then contrasts between the predicted opening angle in the adiabatic and radiative limits, for both mixed and unmixed winds, focus squarely on the effects of adiabaticity, and guide more complete hydrodynamic studies of these differences.

In the process, we also seek to clarify some potential misconceptions about the relative importance of the history of the mass-loading of the shocked region, as opposed to the local constraints stemming from the collision of two individual windstreams without consideration of that history. These issues relate to the concept of centrifugal corrections and the “Dyson approximation” (Dyson 1975), so we begin our analysis there.

1.2. The role of centrifugal corrections

An approximation that has been applied in many contexts (e.g., Luo, McCray, & Mac Low 1990; Stevens et al. 1992; Antokhin, Owocki, & Brown 2004) to highly supersonic bow shocks, is requiring a balance between the ram pressure perpendicular to the shock front in the local colliding windstreams (Dyson 1975). This amounts to neglecting the momentum requirements of *turning* the inertial flow already moving along the shock front, so is termed the neglect of “centrifugal” corrections. Explorations into the errors introduced by this approach (e.g., Mac Low et al. 1991) typically focus on the behavior near the head of the bow shock and on the generation of the hardest X-rays, but the approximation may lose validity farther downstream where the global shock morphology is determined.

It will be argued here that although this approximation is generally valid near the stagnation point, since there the history of the introduction of mass into the shocked region is of least importance, it is not a particularly useful approximation to apply to the *asymptotic* shape of the shock, as the latter is more related to globally integrated geometric factors that incorporate the history of the mass loading of the shock. As such, the Dyson approximation is of more value for analyzing high-temperature emissions from near the shock apex, than it is useful for understanding the more global shock-cone shape. On the other hand, the global character of our approach cannot produce local emission diagnostics near the shock apex, so is intended to be *complementary* to the use of the Dyson approximation, and applicable only to morphological observations.

The key global constraint is overall conservation of the components of vector momentum flux, tracking the wind inputs as well as any external exchange of momentum, in axial wedges conforming to the assumed azimuthal symmetry. The symmetry axis is taken to be the binary line of centers, so applies only on scales where the orbital effects which break that symmetry may be neglected. As will become more apparent below, tracking the global momentum flux is substantially different

from asserting local perpendicular ram balance, because the shocked gas carries a momentum flux that must be *deflected* more so than *stopped*, thereby “soaking up” locally unbalanced ram pressure, as the shock angle turns from its initially perpendicular angle to its ultimate asymptotic angle. This effect represents a type of mass loading, wherein the stronger wind piles into previously shocked elements of *itself*, and that allows for both global and local violation of the perpendicular ram balance. This integrated memory of the interaction, not local physics, determines the asymptotic opening angle of the shock. As such, this paper explores the fundamental *conceptual* reason why the Dyson approximation is not suited to the asymptotic shock geometry, and why this is further exacerbated in the presence of adiabaticity.

2. The formulation of the problem

In this paper we consider two highly supersonic spherically diverging constant-velocity winds colliding along an axis of symmetry in a long-period binary system. For simplicity, both winds are assumed to have reached their terminal speed, and we include no dynamical influences, such as radiative forces or gravity from either star, nor any orbital effects such as coriolis effects or ellipticity (for a study of these latter effects, see Lemaster, Stone, & Gardiner 2007). We also assume that the stellar separation is sufficient such that a normal stagnation point is achieved between the stars—Luo et al. (1990) and CRW looked at what happens when one wind impinges directly on the companion photosphere, but complications ensue and this is not an entirely solved problem.

The star in the binary with the stronger wind momentum flux, if they are not equal, is termed star A, and the weaker is termed star B. The goal is to derive the momentum-flux ratio, η , of the weak-wind star B to the strong-wind star A, that is required to support a given observed asymptotic shock-cone half-angle θ_s , given various assumptions about the interactions such as if they are radiative versus adiabatic, or mixing versus nonmixing. The key parameters to track are the global fluxes of vector momentum and scalar energy, in a manner similar to the approach pioneered for interstellar medium collisions by Wilkin (1996). That approach was updated for spherically diverging winds by CRW, and our main contribution here is the extension to the adiabatic case. This requires that we track the momentum-flux implications of the gas pressure and turbulent pressure (which we will treat as gas pressure), induced by the supersonic collision.

In axial symmetry, the independent domain to understand is an infinitely long and narrow wedge of axial angular thickness $d\phi$ whose vertex is all along the binary line of centers. This wedge is cut into two pieces by the internal working surface of the shock cone between the winds, and all the shocked material is assumed to issue out asymptotically along a single characteristic direction that divides the pieces. We term this the “characteristic-angle” approximation to distinguish it from the thin-shock approximation, which assumes rapid cooling and explicitly neglects all influences of gas pressure. Comeron & Kaper (1998) also relax the requirement of complete radiative cooling, as applied to wind/ISM interactions, but do not take the global approach of following the self-consistent gas pressure influences on the momentum fluxes.

The sources of momentum fluxes in the wedge are the winds of the two stars, and the combined result is treated as if it issued from a single point seen from large distance. As such, we do not include the innovation of CRW of including the angular momentum flux to track the curving shape of the shock front, as we consider the asymptotic domain where the binary system is effectively resolved into a single point and the angular momentum flux vanishes. The sole sink of momentum flux is advection through the outer edge of the wedge at large distances, treated in steady state.

2.1. The characteristic shock-angle approximation

Our core assumption, for the purposes of achieving simple closed-form results, is that the flow of the shocked gas is governed by a single characteristic angle, θ_s , which forms the separatrix of the two winds downstream of the interaction region. Then θ_s is interpreted as the opening half-angle of the asymptotic bow shock, to within the limitations of the approximation. This is also the formal limit considered by CRW, which they justify by assuming rapid radiative cooling and lateral confinement of the shocked gas between the two unshocked winds. When gas pressure is significant, as with adiabatic shocks, such lateral confinement is not physically realizable, but nevertheless the return of thermal energy to bulk flow energy, endemic to adiabatic cooling, is assumed to result in the bulk of the interacting gas exiting the system more or less along a single most prominent or characteristic direction. Future hydrodynamic simulations are planned to explore the applicability of this approximation, but at this stage we view it primarily as a benchmark, intended for systematic comparison between radiative and adiabatic shocks that support a characteristic asymptotic opening angle.

2.2. Solution strategy

We now lay out our fundamental treatment of the quasi-thin shock approximation, in terms of conserved fluxes of vector momentum components in the z and ρ directions. The key addition to the CRW treatment is the inclusion of gas pressure, capable of generating a new source of momentum flux away from the binary line of centers, as occurs in the adiabatic limit. In axial symmetry, gas pressure does not alter the integrated z component of momentum flux within each axial wedge under consideration, because the z direction is globally constant in cylindrical coordinates, and there are no external forces in the z direction. However, gas pressure in the shocked gas can and does increase the flux of the component of momentum that points perpendicular to the axis, which we denote as the ρ direction in cylindrical coordinates. It is this accounting of the ρ component of the momentum flux that allows us to track the influences of adiabaticity.

We consider a sphere at very large radius centered on the binary system, and track the flux in the colliding winds of various scalar and momentum quantities through that sphere. Owing to the axial symmetry, we may restrict to a thin wedge, of axial angular width $d\phi$ and with its

vertex all along the line of centers of the binary, shaped like the section of an orange. Considering such identical wedges avoids cancellation when summing the flux of vectors with ρ components. We may then apply appropriate global conservation laws, resulting from the given flux sources in the spherical winds of each star, and the absence of any external forces (for simplicity we neglect gravity and radiative forces and assume the winds appear at their terminal speeds), to constrain the nature of the fluxes through the sphere, independently of any wind/wind interaction. Hence we obtain quantities that must be the same in the actual case as they are in an imaginary case where the winds do not interact at all, and these quantities supply us with suitable constraints for deriving the desired expression for the characteristic shock angle θ_s .

2.3. Basic definitions

As mentioned above, we define the characteristic angle along which the shocked gas flows to be θ_s , and let P_s be the scalar momentum flux along that angle (a sum over both shocked winds). Purely for convenience we normalize the scalar momentum flux of star A, which is the mass-loss rate \dot{M} times the terminal speed v_A , to be 8π . As all momentum fluxes in this paper are expressed per angular width $d\phi$ of the azimuthal wedge under consideration, this implies that they may all be converted to real momentum flux units by multiplying them by $\dot{M}_A v_A d\phi / 8\pi$.

The essential device we use is to consider separately the flux of the component of momentum in the z direction (i.e., the component along the binary line of centers), the flux of the component of momentum in the ρ direction (along the radius of the wedge), and where possible, the scalar momentum flux (the flux of the magnitude of the momentum being advected). Due to the absence of any external forces on the wedge in the z direction, we may assert equality of the flux of the z component of momentum, between the actual wedge, and an imaginary wedge where no wind interactions of any kind occur. This conservation of z -component of momentum is written

$$P_s \cos \theta_s = P_{A,z}(\theta_s) + P_{B,z}(\theta_s) , \quad (1)$$

where again P_s is the scalar momentum flux of both winds along θ_s , and here $P_{A,z}(\theta_s)$ and $P_{B,z}(\theta_s)$ are

$$P_{A,z}(\theta_s) = 2 \int_0^{\theta_s} d\theta \sin \theta \cos \theta = \sin^2 \theta_s \quad (2)$$

and

$$P_{B,z}(\theta_s) = -2 \int_{\theta_s}^{\pi} d\theta \sin \theta \cos \theta = -\eta \sin^2 \theta_s , \quad (3)$$

which are respectively the flux of the z component of momentum that is embroiled in the shock from wind A and from wind B, for η the ratio of the total wind momentum fluxes in the weak wind (B) to the strong wind (A).

The situation in the ρ direction is altered in a significant way by the potential presence of gas pressure in the shocked winds. Due to the azimuthal symmetry, the pressure may be treated as

an equal squeezing force on opposite faces of the wedge, which when added vectorially, must yield a net flux of momentum in the ρ direction. Let this source of ρ momentum, per angular width $d\phi$, be denoted P_e . Then in a similar spirit to eq. (1), we have for the flux of the ρ component of momentum

$$P_s \sin \theta_s = P_{A,\rho}(\theta_s) + P_{B,\rho}(\theta_s) + P_e , \quad (4)$$

where here

$$P_{A,\rho}(\theta_s) = 2 \int_0^{\theta_s} d\theta \sin^2 \theta = \theta_s - \sin \theta_s \cos \theta_s \quad (5)$$

and

$$P_{B,\rho}(\theta_s) = 2 \int_{\theta_s}^{\pi} d\theta \sin^2 \theta = \eta(\pi - \theta_s + \sin \theta_s \cos \theta_s) . \quad (6)$$

give the sources of ρ momentum from the two winds respectively, again integrated over the solid angle of embroiled gas appropriate for each wind.

It may at first glance seem that the P_e momentum flux in the ρ direction appears somewhat magically, but it can be physically traced to the curved axial symmetry, because the azimuthal transport of vector momentum flux endemic to the high gas pressure in an adiabatic shock will inevitably lead to an enhancement of momentum flux in the ρ direction. This is similar to the way a billiard ball karoming around the edges of a circular table exerts a continuous radially outward force.

Equations (1) and (4) may be viewed as a matrix equation in (η, P_s) in terms of the unknown P_e and the given θ_s , which solves to

$$\eta = \frac{\sin \theta_s - (P_e + \theta_s) \cos \theta_s}{\sin \theta_s + (\pi - \theta_s) \cos \theta_s} \quad (7)$$

and

$$P_s = \frac{(\pi + P_e) \sin^2 \theta_s}{\sin \theta_s + (\pi - \theta_s) \cos \theta_s} . \quad (8)$$

If we imagine that θ_s is known from observation, then the above represents two equations in the three unknowns η , P_s , and P_e , so solving them will require an auxiliary assumption about the energy transport. We will address that assumption in the form of limiting cases that deal with the degree of adiabaticity and the degree of wind mixing.

3. The role of adiabaticity and mixing

Our next requirement is to find appropriate constraints on the scalar energy flux along θ_s to determine the appropriate value for P_e , which in turn gives us our fundamental goal, $\eta(\theta_s)$, via eq. (7). We can do this most easily if we consider the limiting cases of radiative shocks, adiabatic shocks with no mixing, and adiabatic shocks with complete mixing. We shall see that this lists these effects in order of increasingly explosive support of the bow-shock angle (and therefore in descending order of the required value of η).

3.1. Radiative shocks

We first consider the simplest case of purely radiative shocks, for which gas pressure plays no role and we may set $P_e = 0$. This situation is handled in CRW; we include it here only for completeness. The solution from eq. (7) is immediately

$$\eta = \frac{\tan \theta_s - \theta_s}{\tan \theta_s - \theta_s + \pi}. \quad (9)$$

Note that it is not necessary to make any assumptions about the degree of mixing in the two shocked winds, nor to what extent P_s is locally carried by a single speed or a spread in speeds within the shock, because our result for θ_s is a global attribute of the momentum balance independently of how that momentum is partitioned among shock components. The resulting $\eta(\theta_s)$ is depicted in Fig. 1.

3.2. Adiabatic shocks with no mixing

We assume that quasi-thin adiabatic shocks will ultimately convert all the heat thermalized in the shock back into bulk kinetic energy flowing approximately along θ_s , but the impact on P_s will depend on whether the two winds mix and reach a single combined velocity, or if they retain their individual character and return only to their original terminal speed, or some combination thereof. First we treat the case where each wind returns adiabatically to its original terminal speed without mixing. This means that the scalar momentum flux missing from the two original winds will all show up in the asymptotic flow along the shock angle, i.e., that scalar momentum flux will all end up being P_s . Hence instead of substituting for P_e directly, we may replace eq. (4) with the constraint

$$P_s = 2 \int_0^{\theta_s} d\theta \sin \theta + 2\eta \int_{\theta_s}^{\pi} d\theta \sin \theta = 2(1 - \cos \theta_s) + 2\eta(1 + \cos \theta_s). \quad (10)$$

This results in the solutions to eqs. (7) and (8) becoming

$$\eta = \tan^4 \left(\frac{\theta_s}{2} \right) \quad (11)$$

and

$$P_s = 2(1 - \cos \theta_s) + 2 \tan^4 \left(\frac{\theta_s}{2} \right) (1 + \cos \theta_s), \quad (12)$$

subject to

$$P_e = \frac{1}{8} \sec^4 \left(\frac{\theta_s}{2} \right) [8 \sin \theta_s - \pi \cos(2\theta_s) + 4(\pi - 2\theta_s) \cos \theta_s - 3\pi]. \quad (13)$$

The resulting $\eta(\theta_s)$ is depicted in Fig. 1.

3.3. Adiabatic shocks with complete mixing

If we make the opposite assumption that when the thermalized energy is adiabatically returned to the flow along θ_s , the winds are completely mixed and reach a single joint characteristic velocity, then we get the maximal explosive support of the opening angle θ_s . The additional support comes from the fact that not only is the ram pressure perpendicular to the shock thermalized, but even some of the ram pressure initially *along* the shock is thermalized, when the winds mix and reach a common speed. This is essentially an increase in gas pressure due to frictional heating, and so we expect the smallest $\eta(\theta_s)$ in this case. Here our global constraint on P_s comes from the total scalar kinetic energy flux and the total scalar mass flux that enter the shock zone, which must in turn flow out at a single characteristic speed, approximately along θ_s , in a manner consistent with P_s .

Following this logic, the scalar mass flux per wedge thickness $d\phi$, again in units where the total scalar momentum flux from star A is 8π , is

$$M_s = \frac{2}{v_A}(1 - \cos \theta_s) + \frac{2\eta}{v_B}(1 + \cos \theta_s), \quad (14)$$

and the scalar kinetic energy flux in those units is

$$K_s = \frac{P_s^2}{2M_s} = (1 - \cos \theta_s)v_A + \eta(1 + \cos \theta_s)v_B \quad (15)$$

which results in the constraint

$$P_s = 2\sqrt{[1 - \cos \theta_s + (1 + \cos \theta_s)\eta u][1 - \cos \theta_s + (1 + \cos \theta_s)\frac{\eta}{u}]}, \quad (16)$$

where we have defined $u = v_A/v_B$. Applying eqs. (7) and (8) then gives

$$\eta = \frac{\cos^2 \theta_s}{8u(3 \cos \theta_s - 1)} \sec^6 \left(\frac{\theta_s}{2} \right) [2(1 + u^2) \cos^2 \theta_s - 2(1 + u^2) - u \sin^2 \theta_s \tan^2 \theta_s + \sqrt{2} \sqrt{1 + u + 4u^2 + u^3 + u^4 + (1 - u)^2(1 + u + u^2) \cos(2\theta_s) \sin \theta_s \tan \theta_s}], \quad (17)$$

and the expressions for P_s and P_e may also be written in closed form but they are quite long and involved. Although it is not immediately obvious, the result in eq. (17) does indeed reduce to eq. (11) when $u = 1$, since then the presence or absence of mixing is irrelevant to the global dynamics. This result for $\eta(\theta_s)$ is also included in Fig. 1.

4. Discussion

Our fundamental result is that an increased flux of the momentum component away from the axis is generated by the extreme heating of the shocked gas, and this can substantially widen the asymptotic bow shock angle as seen in Fig. 1. It is also clear that the bow shock angle reaches 90° when $\eta = 1$ for any of the limits of radiative or adiabatic cooling, as would be expected from

symmetry requirements. The figure shows that for asymptotic opening half-angles of roughly 50 degrees, for example, adiabaticity roughly halves the weak-wind momentum flux required to support that shock geometry, and if winds with a fairly extreme factor 4 contrast in terminal speeds are mixed, it will halve the requirement yet again. Indeed, the results from eqs. (9), (11), and (17) give that the required η for a 50 degree asymptotic half-angle are 0.1, 0.05, and 0.027 respectively. The physical source of these differences can be traced in a schematic yet quantitative way by examining scaling laws generated in the limit $\eta \ll 1$, as we analyze next.

4.1. Winds with extremely low momentum-flux ratio

The above results simplify in the limit $\theta_s \ll 1$, which occurs when $\eta \ll 1$, so it is informative to consider what physical insights may be conferred in that simple limit. Note these limits apply asymptotically only when the weak-wind star has a negligibly small radius; in real situations, when η is small enough for asymptotic expressions to apply, the possibility must be considered separately that the strong wind may crash directly into the photosphere of the companion, invalidating our assumptions. Nevertheless, the low- η limits do convey general insights into the reasons that different degrees of adiabaticity require different amounts of weak-wind momentum to support the shock cone at a given opening angle θ_s , and it is one of the primary advantages of closed-form expressions that they submit to this type of scaling analysis.

We begin by noting that if one adopts the local approximation of equating the perpendicular momentum fluxes across the shock front (e.g., Dyson 1975; Luo et al. 1990; Stevens et al. 1992; Antokhin et al. 2004; Falceta-Goncalves, Abraham, & Jatenco-Pereira 2008) and extrapolates it globally to the asymptotic opening angle, one should expect the required η to scale like θ_s^2 when $\theta_s \ll 1$. This is because the strong wind effectively has no inertia after it is shocked, so the weak wind bears the full burden at every point along the shock of maintaining that shock against the strong wind ram pressure. The weaker wind can maintain a perpendicular ram balance against at most a solid-angle fraction of order η of the strong wind, and θ_s^2 determines the solid-angle fraction subtended by the interaction zone, so $\eta \propto \theta_s^2$.

However, when a more accurate global accounting of the momentum requirements is undertaken, in the limit of radiative shocks we find from eq. (9) that

$$\eta \cong \frac{\theta_s^3}{3\pi}, \quad (18)$$

as seen in the exact result of CRW and the heuristic fit of Eichler & Usov (2003). The extra power of θ_s may be interpreted as being due to the fact that the global requirement for the weak wind is not to *stop* the strong wind, but merely to *deflect* it through an angle θ_s . So the η momentum flux must deflect through an angle θ_s a fraction $\sim \theta_s^2$ of the strong wind, requiring $\eta \sim \theta_s^3$. Indeed, we can be even more quantitative and note that the strong-wind momentum flux along the z direction is $2 \int_0^{\theta_s} d\theta \sin \theta \cos \theta \cong \theta_s^2$, and the deflecting momentum flux in the ρ direction from the weak

wind is $2\eta \int_{\theta_s}^{\pi} d\theta \sin^2 \theta \cong \pi\eta$, along with a contribution in the ρ direction from the strong wind itself of $2 \int_0^{\theta_s} d\theta \sin^2 \theta \cong 2\theta_s^3/3$. Adding the momentum flux in the ρ direction to that in the z direction bends the total shocked momentum flux an angle θ_s , where from the above estimates we have

$$\theta_s \cong \frac{\pi\eta}{\theta_s^2} + \frac{2\theta_s^3}{3\theta_s^2}, \quad (19)$$

which results directly in $\eta \cong \theta_s^3/3\pi$.

For adiabatic shocks with no mixing, our approximation in eq. (11) yields when $\theta_s \ll 1$

$$\eta \cong \frac{\theta_s^4}{16}. \quad (20)$$

Here we find yet another added power of θ_s , this time because the explosive heating of the shocked winds, upon re-expansion away from the axis, provides substantial momentum support for the bending of the shock angle. Indeed, the combination of the pre-shocked momentum flux in the ρ direction, and the explosive gas pressure contribution in that direction, produce *almost* enough momentum to support a small deflection θ_s by themselves, without help from the weak wind. Hence the weak wind needs to provide only a small “coaxing” on top of these two momentum fluxes along ρ (each which scales $\sim \theta_s^3$), so this coaxing appears at an even higher order of θ_s , at order θ_s^4 . So this analysis elucidates the physical reasons why radiative shocks require less weak-wind momentum flux to maintain a given narrow shock angle than would a putative perpendicular ram balance, and adiabatic shocks require less still.

Considering the case of adiabatic shocks with complete mixing, we find from eq. (17) that when $\theta_s \ll 1$,

$$\eta \cong \frac{\theta_s^4 u}{8(1+u^2)}, \quad (21)$$

where again u is the ratio of the terminal speeds in the two winds, and it does not matter which wind is in the numerator, only the contrast expressed by u . Here we see the now-familiar θ^4 scaling of adiabatic shocks, but we also find that when there is a strong contrast in the wind speeds, adiabatic mixing allows additional thermalization and additional explosive expansion away from the axis, further supporting the deflection of the strong wind and allowing for an even smaller η to suffice, in light of the identity $u/8(1+u^2) < 1/16$.

5. Conclusions

We use global momentum-flux considerations in the context of a characteristic-angle shock approximation to derive the resulting asymptotic opening angle of shocked gas for two colliding spherical winds, for either fast or slow radiative cooling, with complete or limited mixing. Hence this may be viewed as an extension of the CRW approach to global shock characteristics in the presence of significant adiabatic cooling. For intermediate levels of adiabaticity and mixing, informal

interpolation of our results would seem preferable to an effort to track the transitional physics in detail, given the rough character of the approximations used.

We find that adiabaticity measurably widens the asymptotic characteristic angle of the wind interaction, or for a fixed observed opening angle, significantly reduces the associated wind momentum-flux ratio that would support it, as described in eqs. (9) and (11). Mixing of winds with different terminal speeds would have no additional effect in the radiative limit, but in the adiabatic limit further reduces the inferred wind momentum-flux ratio, as seen in eq. (17). Hence, the observed angle, the wind momentum-flux ratio, and the degree of adiabaticity and mixing, all form a set of parameters that permit knowledge about some to be used to infer or constrain the others. In particular, observations of the characteristic wind interaction angle, whether from spectra or visible dust formation, can be used to draw inferences about the character of the colliding winds.

The nature of the approximation is certainly highly idealized, as radiative shocks are subject to shear instabilities, adiabatic shocks suffer explosive spreading of the shocked gas, and mixing can result in a range of flow speeds instead of a single uniform one, so our approximation faces significant limitations in practice. Also, clumping in the wind might present additional challenges (although Pittard 2007 finds that clump winds collide in a broadly similar way to smooth winds). Overall, the goal is to provide a straightforward way to obtain analytic closed-form expressions which elucidate certain basic physical differences, which are intended to inform a new vocabulary for unifying the discussion around hydrodynamic simulations of wind/wind collisions over a wide range of circumstances. Future hydrodynamical simulations will be needed to investigate the proper interpretation of the concept of a characteristic quasi-thin shock angle, in the face of realistic complications in that idealization.

For example, Pilyugin & Usov (2007) find that equal-strength adiabatic winds collide in such a way as to generate so much pressure-driven expansion of the shock region that ultimately both winds are entirely embroiled. Nevertheless, we point out that once the gas adiabatically cools and returns to some approximation of its original terminal speed, a prevailing feature will be the contact discontinuity along the central plane, and that is where our analysis would locate the “characteristic angle” of the interaction for equal winds. So even when a thin shocked layer is not physically realized, there may yet be value in thinking in terms of global momentum considerations and characteristic interaction angles.

Thus our approximate results are here intended to provide a benchmark against which to compare and interpret more detailed simulations, moreso than as a quantitatively accurate description of the detailed nature of the wind interaction. For highly unequal winds, the most natural interpretation of the derived angle will be the working surface in the stronger wind, but detailed simulations are needed to verify this expectation. Since the greater the adiabaticity, the wider the characteristic angle (especially for strong mixing), these results are intended to help form expectations about the influences of adiabaticity and mixing on any particular observed bow-shock geometry, especially at early stages of the analysis when few constraints on the wind collision may

easily be determined. Disentangling the independent parameters of mass and momentum fluxes in colliding winds benefits from consideration of all possible diagnostic constraints, and the global treatment here may be used to complement more detailed studies of the interaction closer to the stagnation zone.

References

- Antokhin, I. I., Owocki, S. P., & Brown, J. C. 2004, *ApJ*, 611, 434
- Eichler, D. & Usov, V. 1993, *ApJ*, 402, 271
- Canto, J., Raga, A. C., & Wilkin, F. P. 1996, *ApJ*, 469, 729
- Comeron, F. & Kaper, L. 1998, *A&A*, 338, 273
- Dyson, J. 1975, *Ap&SS*, 35, 299
- Falceta-Goncalves, D., Abraham, Z., & Jatenco-Pereira, V. *MNRAS*, 2008, 383, 258
- Girard, T. & Willson, L. A. 1987, *A&A*, 183, 247
- Hill, G. M., Moffat, A. F. J., & St-Louis, N. 2002, *MNRAS*, 335, 1069
- Ignace, R., Bessey, R., & Price, C. S. 2009, *MNRAS*, 395, 962
- Lemaster, M. N., Stone, J., M., & Gardiner, T. A. 2007, *ApJ*, 662, 582
- Luhrs, S. 1997, *PASP*, 109, 504
- Luo, D., McCray, R. & Mac Low, M.-M. 1990, *ApJ*, 362, 267
- Mac Low, M.-M., Van Buren, D., Wood, D. O. S., & Churchwell, E. 1991, *ApJ*, 369, 395
- Pilyugin, N. N. & Usov, V. V. 2007, *ApJ*, 655, 1002
- Pittard, J. 2007, *ApJ*, 660, L141
- Rauw, G., Crowther, P. A., De Becker, M., Gosset, E., Naze, Y., Sana, H., van der Hucht, K. A., Vreux, J.-M., & Williams, P. M. 2005, *A&A*, 432, 985
- Shore, S. N. & Brown, D. N. 1988, *ApJ*, 334, 1021
- Stevens, I. R., Blondin, J. M., & Pollock, A. M. T. 1992, *ApJ*, 386, 265
- St-Louis, N., Moffat, A. F. J., Marchenko, S., & Pittard, J. 2005, *ApJ*, 628, 953
- St-Louis, N., Willis, A. J., & Stevens, I. R., 1993, *ApJ*, 415, 298
- Tuthill, P. G., Monnier, J. D., Lawrance, N., Danchi, W. C., Owocki, S. P., & Gayley, K. G. 2008, *ApJ*, 675, 698

Tuthill, P. G., Monnier, J. D., Tanner, A., Figer, D., Ghez, A., & Danchi, W. 2006, *Sci*, 313, 935

Wilkin, F. P. 1996, *ApJ*, 459, L31

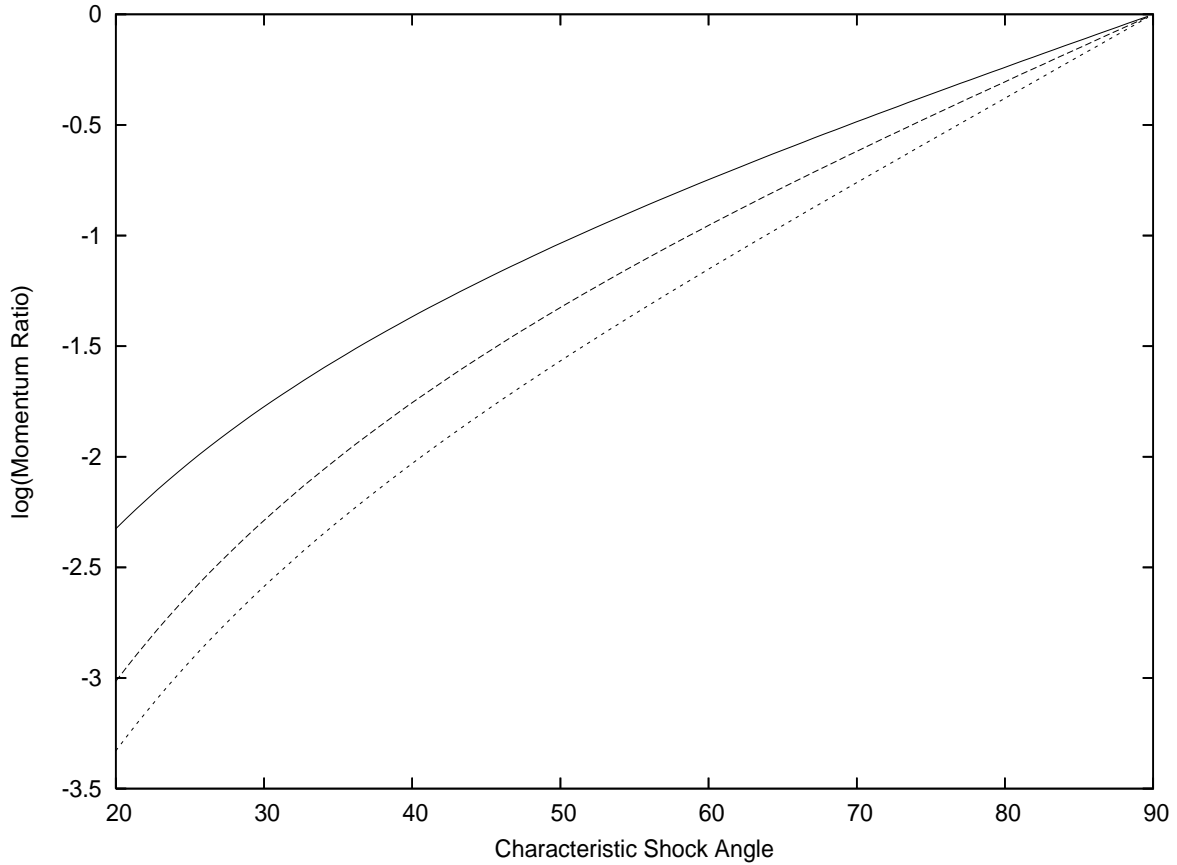


Fig. 1.— The log (base 10) of the wind momentum ratio η that would be necessary to sustain a characteristic shock angle θ_s (in degrees), for radiative shocks (solid curve), adiabatic shocks without mixing (dashed curve), and adiabatic shocks with complete mixing and a terminal speed contrast of $u = 4$ (dotted curve). Note that the possibility of a direct collision with the photosphere of the weak-wind star is not considered, even for small η .